Interband Optical Properties of Grain Boundaries in Germanium: An Amorphous System*

JERROLD L. MCNATT† AND PAUL HANDLER
Departments of Physics, Electrical Engineering, and the Materials Research Laboratory, University of Illinois, Urbana, Illinois 61801
(Received 29 July 1968)

We have measured the interband optical properties of grain boundaries by a spatial-modulation technique which allows direct observation of the differences between the regular lattice and the grain boundary. These results are obtained by periodic motion of the grain boundary in a bicrystal in and out of a narrow light beam and phase-sensitive detection of the difference signal. The grain boundary is found to have an absorption edge which is broadened by the electric fields within the boundary as well as an exponential distribution of states below the direct edge. The results were independent of the tilt axis of the grain boundary (from 4° to 25°) and the data are found to be very similar to those observed for amorphous films of germanium. A 6° twist boundary gave identical results. While this paper is concerned with the properties of a planar defect, we believe the method will also prove useful for the study of point defects in crystals.

I. INTRODUCTION

THE initial observation by Taylor, Odell, and Fan[1] of the current blocking action of the potential barriers at grain boundaries in n-type germanium was followed by studies of current flow both perpendicular[2–4] and parallel[5–9] to the grain-boundary plane and the photoelectric response of the boundary.[10–12] The following are some of the important properties that have been established by these experiments:

(i) Localized states at the grain boundary act as acceptors, resulting in the creation of 10^{12}–10^{13} cm^{-3} mobile holes[7] in the space-charge region adjacent to the grain-boundary region.

(ii) The layer containing these localized states and mobile holes is certainly 1000 Å or less and probably more like 100 Å in thickness.[4]

(iii) The acceptor character of the boundary layer is not affected by the type or concentration of impurities used to dope the bicrystal[3,5,13] and is definitely not associated with impurity precipitation at the boundary.[13]

(iv) The p-type conduction in wide-angle grain-boundary layers shows a variation of only about a factor of 2 in both the number of carriers and their mobility over the temperature range 4.2–240°K.[7,9]

(v) Under illumination of the regions adjacent to the grain boundary a photovoltage is developed. The photovoltage polarity indicates that the boundary layer is p type.[10–12]

(vi) A space charge extends out on both sides of the grain-boundary layer to distances of the order of microns depending on the doping of the bulk material. The maximum electric field in the space-charge layer seems to be of order 10^4–10^5 V/cm.[2]

Most of the electrical measurements have been carried out on carefully grown bicrystals[14] with a simple tilt configuration.

The model employed by several investigators to explain the grain-boundary acceptor nature has been the "dangling bond states" due to the broken covalent bonds at each of the edge dislocations making up a Burgers model[15] of the simple tilt boundary. Although such a model appears well established for low-angle grain boundaries, it appears to be questionable for medium (1°–30°) angles and especially for angles greater than 15°.[16] Bubble-raft studies simulating tilt boundaries in metal crystals show that as the boundary tilt angle increases to about 15°–20°, the boundary can no longer be characterized as a dislocation array but becomes a narrow region of lattice misfit.[17] Many of the germanium bicrystal studies have been carried out on 10°–20° tilt-angle boundaries. Moreover, the covalent bonding in germanium is highly directional in nature.

* Work was supported in part by the Advanced Research Projects Agency under Contract SD-131, the Army Research Office, Durham, and by the Office of Naval Research.

† Present address: Pratt & Whitney Aircraft, Middletown, Conn. 06458.

[1] W. E. Taylor, H. H. Odell, and H. Y. Fan, Phys. Rev. **88**, 867 (1952).

[2] R. K. Mueller, J. Appl. Phys. **32**, 635 (1961).

[3] R. K. Mueller, J. Appl. Phys. **32**, 640 (1961).

[4] H. F. Mataré, in *Solid State Physics in Electronics and Telecommunications*, edited by M. Desirant and J. L. Michiels (Academic Press Inc., New York, 1960).

[5] B. Reed, O. A. Weinreich, and H. F. Mataré, Phys. Rev. **113**, 454 (1959).

[6] A. G. Tweet, Phys. Rev. **99**, 1182 (1955).

[7] G. Landwehr and P. Handler, J. Phys. Chem. Solids **23**, 891 (1962).

[8] Y. Matukura, J. Phys. Soc. Japan **17**, 1405 (1962).

[9] Y. Hamakawa and J. Yamaguchi, Japan J. Appl. Phys. **1**, 334 (1962).

[10] O. Weinreich, H. F. Mataré, and B. Reed, in *Solid State Physics in Electronics and Telecommunications*, edited by M. Desirant and J. L. Michiels (Academic Press Inc., New York, 1960).

[11] H. F. Mataré, D. C. Cronemeyer, and M. W. Beaubien, Solid State Electron. **7**, 583 (1964).

[12] W. W. Lindemann and R. K. Mueller, J. Appl. Phys. **31**, 1746 (1960).

[13] R. K. Mueller, J. Appl. Phys. **30**, 546 (1959).

[14] H. F. Mataré and H. A. R. Wegener, Z. Physik **148**, 631 (1957).

[15] J. M. Burgers, Proc. Koninkl. Ned. Akad. Watenschap **42**, 293 (1939); **42**, 378 (1939).

[16] R. S. Wagner and B. Chalmers, J. Appl. Phys. **31**, 581 (1960).

[17] S. Amelinckx and W. Dekeyser, Solid State Phys. **8**, 325 (1959).

The formation of the highly deformed bonds required for a dislocation array model will require hybridization with states of higher energy. Thus, more complicated structures involving less bond deformation should become energetically more favorable at low tilt angles. Finally, the simplest dislocation array model for a pure twist boundary is an array of screw dislocations having no broken bonds and hence no acceptor states.[3] However, the electrical properties of pure twist boundaries are very similar to those of pure tilt boundaries even for angles of twist as low as 6°.[3,8]

Thus, the often-employed simple dislocation array model should be replaced by more realistic structures like islands of lattice fit and misfit[18] or a plane of simply connected voids.[19] Another option is one of several two-dimensional dislocation array models.[17] In these cases there is less deformation per bond and the acceptor states can be attributed to unbonded orbitals at misfit islands or voids.

Taking another point of view, Heine[20,21] has pointed out that at a surface of discontinuity in the crystal potential (like a surface or grain boundary) one must match the electron wave functions at the boundary using an infinite set of solutions of the Schrödinger equation. This series includes the Tamm evanescent or surface waves of energy E which decay exponentially away from the boundary as well as the Bloch waves of energy E, if they exist. For some values of energy, E, solutions may exist which are composed entirely of evanescent waves, that is, localized states exist at the boundary. Since the exact structure of the grain boundary is uncertain and therefore the potential to be used is unknown, it is only possible to make qualitative predictions about the energy-level diagram.

Usually optical measurements are one of the most promising sources of data from which models of energy-level structure can be derived. However, in the case of bicrystals, the grain-boundary optical absorption has up to now not been observed directly. This is due to the fact that the atoms in the grain-boundary layer form a very small fraction of the total number of atoms in the region illuminated by an incident light beam. Optical studies have been confined to measurements of photoresponse spectra. The photoresponse is a combination of the effects of electron-hole pair creation in the bulk semiconductor followed by collection of holes by the grain boundary and perhaps also a small contribution due to absorption processes in the grain-boundary layer. Mataré and co-workers[11] found that the germanium grain boundary broadens the energy range of the photoresponse as compared with other junction devices in single crystals of the same material. From their data, they concluded that the grain boundary possesses a midband state which lies about 0.42 eV from one of the band edges. Lindemann and Mueller[12] observed two small irregularities in bicrystal photoresponse curves at 0.745 and 0.72 eV at liquid-N_2 temperatures which were tentatively assigned to grain-boundary levels.

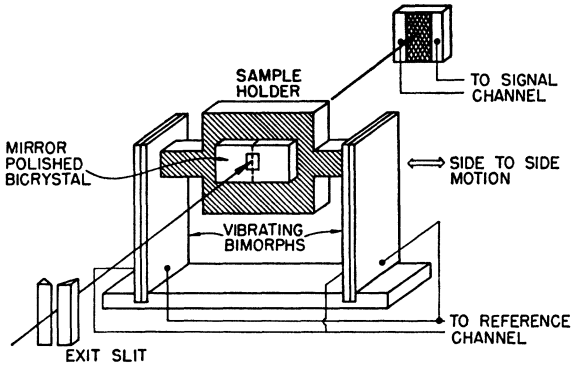

FIG. 1. Bicrystal sample mount for spatial-modulation measurements.

In this paper we report measurements of the optical absorption associated with grain boundaries in n-type germanium in the range 1–2.5 μ (0.5–0.8 eV), using a technique which permits more direct observation of the optical absorption of the grain-boundary layer. The absorption can be divided into at least two contributions: one due to electric field effects in the grain-boundary space-charge layer, and the other to a smearing out of the normal germanium fundamental absorption edge because of the disordered nature of the grain-boundary layer. In Sec. II the experimental techniques are described in detail. In Sec. III the data are presented and in Sec. IV they are discussed.

II. EXPERIMENTAL TECHNIQUES

A. Spatial Modulation

The technique used to examine grain-boundary optical absorption is illustrated in Fig. 1. A monochromatic light beam was focused into a rectangular shape 0.3×3.0 mm^2 on the front surface of the bicrystal sample having mirror-polished front and back surfaces. The bicrystal was mounted in turn between two Clevite bender bimorphs wired to move together when an ac voltage at frequency f_0 is applied to them. The bimorphs are in turn mounted on a motor-driven platform so that the relative position of the grain-boundary plane and light beam can be varied. If the grain-boundary region has optical absorption greater (or less) than the surrounding single-crystal germanium material, a very small ac modulation of the transmitted light, ΔI, occurs when the motion is such that the grain-boundary region periodically moves in and out of the light beam. The transmitted light is focused on a PbS detector which is connected to a PAR HR-8 lock-in amplifier operating at a frequency $2f_0$. Detection at the second harmonic is

[18] N. F. Mott, Proc. Phys. Soc. (London) **60**, 391 (1948).
[19] P. Handler, Ann. Acad. Sci. N. Y. **101**, 857 (1963).
[20] V. Heine, Surface Sci. **2**, 1 (1964).
[21] V. Heine, Proc. Phys. Soc. (London) **81**, 200 (1963).

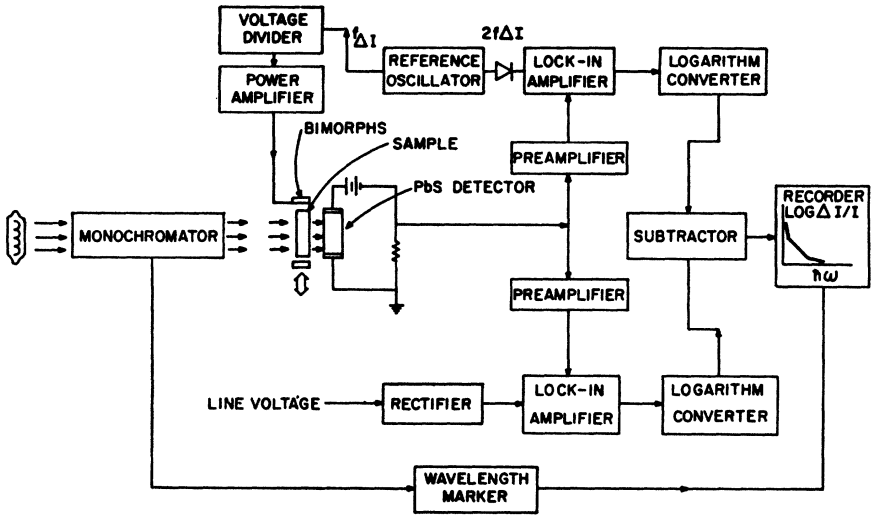

FIG. 2. Block diagram of apparatus.

used to eliminate mechanical and electrical pickup problems.

Simultaneously, the total transmitted light I was also measured using a light chopper and a second lock-in amplifier operating at a different frequency. The ratio was taken using logarithmic conversion. Figure 2 shows a block diagram of the apparatus. The monochromator used was a Perkin-Elmer 210 with a Sylvania sun gun lamp and a Kodak PbS detector.

In Fig. 3 a recording of the ΔI signal detected at the second harmonic as a vibrating bicrystal sample was moved slowly through the light beam is presented. The peak shown locates the grain boundary. Data on the spectral dependence of grain-boundary optical properties was taken with the sample positioned at this peak. The other oscillations seen on this scan were repeatable in successive scans and are probably coming from in-phase signals produced by diffuse scattering (or absorption) of radiation by minute imperfections on the surface or in the bulk. These signals constitute the background and thus limit the sensitivity of the measurements.

In order to keep the aforementioned background as small as possible, the front and back surfaces were polished to a mirror finish using 6-, 1-, and $\frac{1}{4}$-μ diamond pastes and a Buehler Vibroment automatic polishing machine. Electropolishing could not be used since it tended to etch a groove at the grain boundary,[22] making it a source of diffuse scattering of radiation at the surfaces.

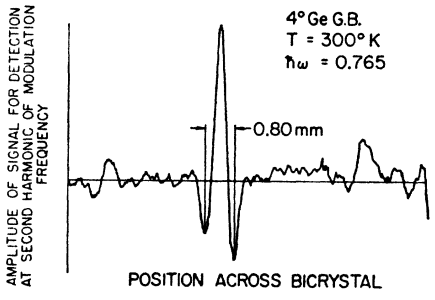

FIG. 3. Second-harmonic signal as light beam is scanned across vibrating bicrystal.

The geometry of these measurements is an important consideration in their interpretation. As illustrated in Fig. 4(a), only a small portion of the light beam actually goes through the grain-boundary region of thickness τ. Moreover, the incoming rays which go through the grain-boundary region make rather large angles with the normal to the grain-boundary plane.

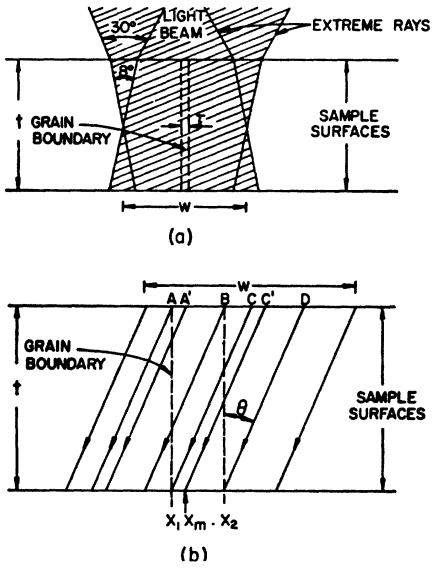

FIG. 4. (a) Cross section of bicrystal showing geometry of light beam when both light beam and grain boundary are normal to crystal surfaces. (b) Parallel bundle of light rays cutting grain-boundary plane at angle θ.

[22] M. V. Sullivan, D. L. Klein, R. M. Finne, L. A. Pompliano, and G. A. Kolb, J. Electrochem. Soc. 110, 412 (1963).

In order to relate the measured values of ΔI and I to the absorption properties of the grain-boundary region, it is easiest to look first at all rays which make an angle θ with grain-boundary plane as shown in Fig. 4(b). The rays which pass through the grain-boundary region (x_1 to x_2) fall into two catagories: those which pass entirely through the region during the whole cycle of motion (between rays B and C) and those which pass through it (between A and B and also between C and D) for only a portion of the cycle of motion. It is convenient to take the latter rays in pairs like A′ and C′.

The normalized change in transmitted intensity produced when the grain boundary is in the light beam consisting entirely of rays at angle θ is

$$\left(\frac{\Delta I}{I}\right)_\theta=\left[\frac{t\tan\theta-\tau}{W}\right]\left(\frac{\Delta I}{I}\right)_{BC}+\frac{\tau}{W}\left(\frac{\Delta I}{I}\right)_{AB,CD}, \quad (1)$$

where W is the width of the light beam. The factors in brackets represent the fraction of the (assumed uniform) light beam in regions BC and AB, CD, respectively [Fig. 4(b)]. The above expression can be put into the following form:

$$\left(\frac{\Delta I}{I}\right)_\theta=\frac{t\tan\theta}{W}\left[\exp\left(-\int_{x_1}^{x_2}\frac{(\langle\alpha(x)\rangle-\alpha)}{\sin\theta}dx\right)-1\right]$$
$$-\frac{1}{W}\int_{x_1}^{x_2}\left[\exp\left(-\int_{x_1}^{x_m}\frac{(\langle\alpha(x)\rangle-\alpha)}{\sin\theta}dx\right)-1\right]$$
$$\times\left[\exp\left(-\int_{x_m}^{x_2}\frac{(\langle\alpha(x)\rangle-\alpha)}{\sin\theta}dx\right)-1\right]dx_m, \quad (2)$$

where x is the coordinate normal to the grain-boundary plane, $\langle\alpha(x)\rangle$ is absorption coefficient of a narrow slab of the grain-boundary region located at position x and averaged over the plane normal to x, and finally α is the bulk germanium absorption coefficient. If the arguments of the exponentials are small, that is, if

$$\frac{\ll\Delta\alpha\gg\tau}{\sin\theta}\equiv\int\frac{(\langle\alpha(x)\rangle-\alpha)}{\sin\theta}dx\ll 1, \quad (3)$$

then the above expression can be simplified by expanding the exponentials and keeping only the linear terms in $\langle\langle\Delta\alpha\rangle\rangle$. Using reasonable values of $\langle\langle\Delta\alpha\rangle\rangle$ and τ one can show that in the spectral region of interest $\langle\langle\Delta\alpha\rangle\rangle\tau<10^{-2}$. For the grain-boundary layer $\tau\approx10^{-6}$ cm and the greatest value of $\langle\langle\Delta\alpha\rangle\rangle$ would be 10^4 cm^{-1}.[23] Thus, if $\sin\theta$ is kept greater than 10^{-2}, the expansion is valid. By cutting the samples so that no ray goes through the boundary region at angles less than 1° or by rotating the sample to accomplish the same end, this condition can be reasonably well satisfied. Using the approximation of Eq. (3), Eq. (2) becomes

$$\left(\frac{\Delta I}{I}\right)_\theta=-\frac{t}{W}\int_{x_1}^{x_2}[\langle\alpha(x)\rangle-\alpha]dx\sec\theta. \quad (4)$$

Integrating over all the angles in the beam gives

$$-\frac{W}{t}\frac{\Delta I}{I}\approx\int_{x_1}^{x_2}[\langle\alpha(x)\rangle-\alpha]dx=\ll\Delta\alpha\gg\tau. \quad (5)$$

Thus, the (averaged over grain-boundary region) difference in absorption coefficient between normal bulk semiconductor and grain-boundary region is measured by taking the measured ratio $\Delta I/I$ at each photon energy.

TABLE I. Bicrystal properties.

Boundary angle and type	Resistivity of host (Ω cm)	Average orientation of growth	Tilt or twist axis	Sample thickness (μ)	Source
4° tilt	5–7	[100]	[100]	320	Hamakawa
6°13′ twist	12–15	[100]	[100]	485	Matukura
12° tilt	0.3–0.5	[100]	[100]	260	Hamakawa
				460	
16° tilt	10–18	[100]	[100]	134	Nucleonic
				1310	Products Inc.
18° tilt	0.3–0.5	[100]	[100]	350	Hamakawa
20° tilt	14–18	[100]	[100]	160	Mueller

B. Electrical Modulation

A second technique which was employed was electrical modulation by which dc and ac biases were applied across the grain-boundary n-p-n structure through Ohmic contacts to the n regions. These biases should lead to changes in the electric fields in the space-charge layers and therefore to variations in grain-boundary absorption. The effect has already been extensively studied in germanium p-n junctions,[24,25] and in an electrical modulation study of the optical properties germanium surface states.[26] The equipment used in these measurements is very similar to that already described in Ref. 24.

III. RESULTS OF SPATIAL MODULATION

Table I gives the physical properties of the germanium bicrystals used. All were Sb-doped n-type crystals grown by the individual or organization cited as source. The 4°, 12°, and 18° tilt boundary bicrystals and the 6°31′ twist boundary bicrystals were prepared using an oriented double seed pulling technique described in detail by Mataré and Wagener.[14] The method

[23] T. P. McLean, Progr. Semicond. 5, 53 (1960).

[24] A. Frova and P. Handler, Phys. Rev. 137, A1857 (1965).

[25] A. Frova, P. Handler, F. A. Germano, and D. E. Aspnes, Phys. Rev. 145, 575 (1966).

[26] G. Chiarotti, G. Del Signore, A. Frova, and G. Samoggia, Nuovo Cimento 26, 403 (1962).

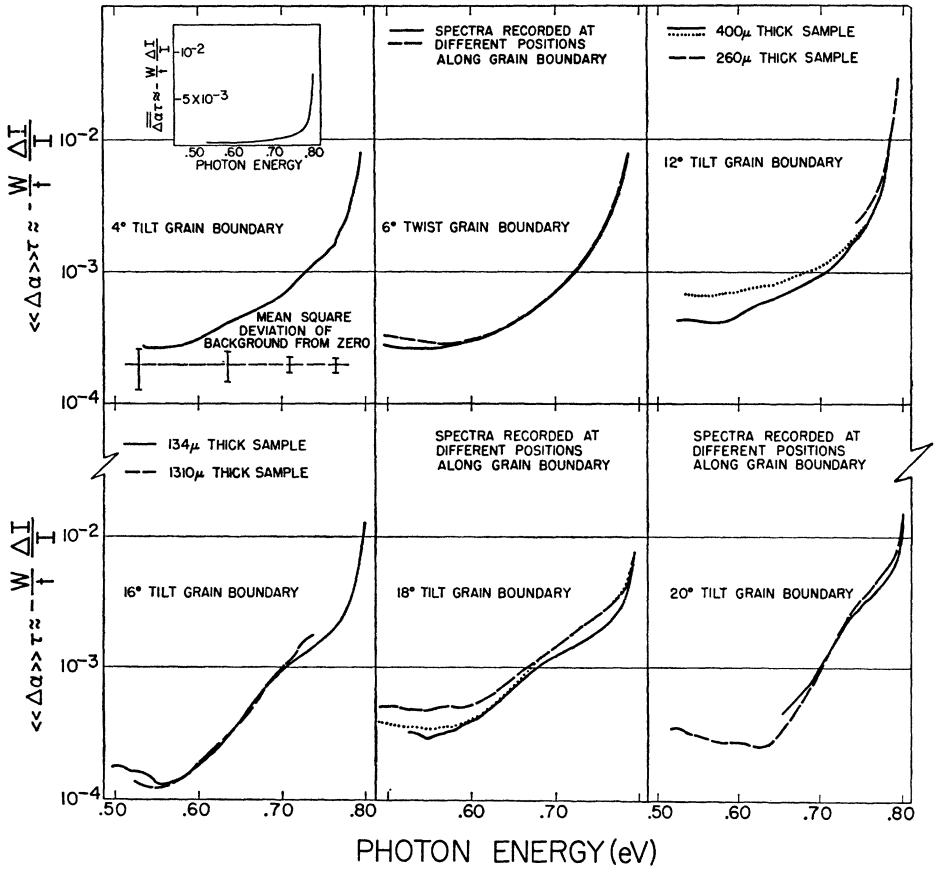

FIG. 5. Spatial-modulation spectra for six bicrystals.

of growth for the others is not known. In some cases several samples from the same bicrystal were polished and measured, whereas in others a large area sample was prepared so that measurements could be made with the light beam scanning different parts of the same bicrystal. Both these means were used to check reproducibility. These several measurements agreed well as to magnitude and shape, indicating that the background signals were not producing significant errors.

Figure 5 represents the spatial-modulation data. For the six different grain boundaries, the results are approximately the same. There is a sharply falling exponential absorption tail directly below the direct edge (~0.80 eV) and a less steep second exponential tail extending from the direct edge to lower energies. Below approximately 0.55–0.60 eV the ΔI signal was approximately equal to background inhomogeneities in the volume or surface of the crystal so that the data below these energies may be uncertain. To determine the source of this excess absorption, a dc electrical bias was applied to the *n-p-n* grain-boundary structure during spatial modulation. Figure 6 shows the results for a tilt as well as a twist boundary. The largest effect of changing the electric field in the space-charge region occurs above 0.75 eV although there are some smaller oscillations in the 0.62–0.76-eV range which are related to the indirect edge in germanium. Similar results were observed for all crystals.

The exponential tail near the direct edge can then be understood as a Franz-Keldysh effect (photon-assisted tunneling) at the direct edge and an estimate of the effective fields present can be made from the electrical modulation data. The oscillation about the indirect edge in Fig. 6 for a 16° tilt boundary are expanded in Fig. 7 and compared with the results for a *p-n* junction. The spectra agree very well in that the transition associated with the LA phonon emission and absorption are located at the same energies. Likewise, the same energies for the LA and TA phonons are read from each measurement. Similar spectra were obtained for all other bicrystals examined by this method. Thus, it appears that the modulation of the potential across the sample causes modulation of the electric fields in the space-charge layer (a region microns in width with the bulk semiconductor band structure) leading to the measured direct and indirect electroabsorption spectra associated with the ordered lattice. There are two discernable differences between the data taken for the two systems. As seen in Fig. 7, the negative peaks of the LA emission and absorption are smaller relative to the positive peaks in the grain-boundary case. Such a trend is toward better agreement with the line shape predicted

by the theory of electroabsorption.[24,25] However, one is probably not measuring the parameter

$$\Delta\alpha(F,\hbar\omega)=\alpha(F,\hbar\omega)-\alpha(0,\hbar\omega) \tag{6}$$

measured in the p-n junction measurements, but rather

$$\Delta\alpha(\langle F_1\rangle,\langle F_2\rangle,\hbar\omega)$$

$$=\int\Big[\alpha[F(V(x)+\Delta V(x))]-\alpha[F(V(x)-\Delta V(x))]\Big]dx$$

$$=\alpha(\langle F_1\rangle,\hbar\omega)-\alpha(\langle F_2\rangle,\hbar\omega), \tag{7}$$

where the $\langle F\rangle$'s represents effective fields in the grain-boundary space-charge layer, the integratings over x are carried out over the space-charge layer, and the electric field distribution in the space-charge layer, $F(V(x))$, may be given by solutions of Poisson's equation similar to those applied to space-charge layers at semiconductor surfaces.[2,27]

The other difference involves the bias dependence of the width of the oscillations of Fig. 7, particularly the width marked Δ. Penchina's theory of indirect absorption[28] predicts that the width Δ should depend on electric field as

$$\Delta\propto F^{2/3}.$$

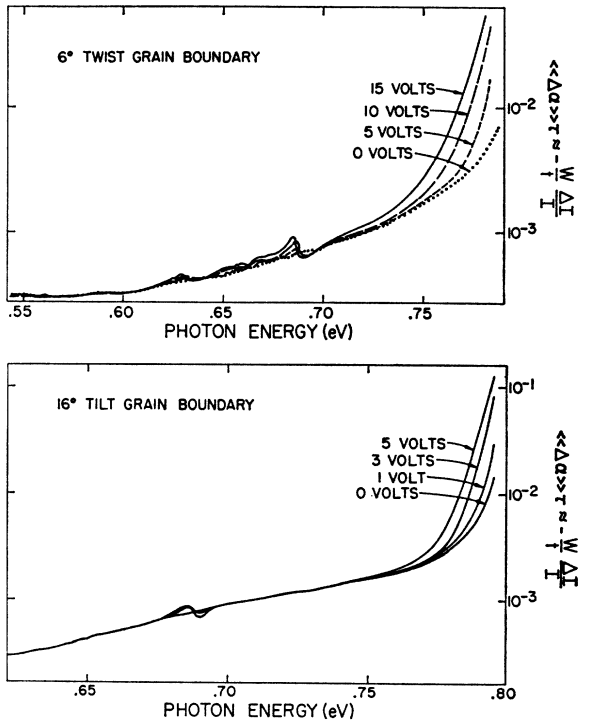

FIG. 6. Effect of dc bias applied across grain-boundary n-p-n structure on spatial-modulation spectra.

[27] R. H. Kingston and S. F. Neustader, J. Appl. Phys. 26, 210 (1955).

[28] C. M. Penchina, Phys. Rev. 138, A924 (1965).

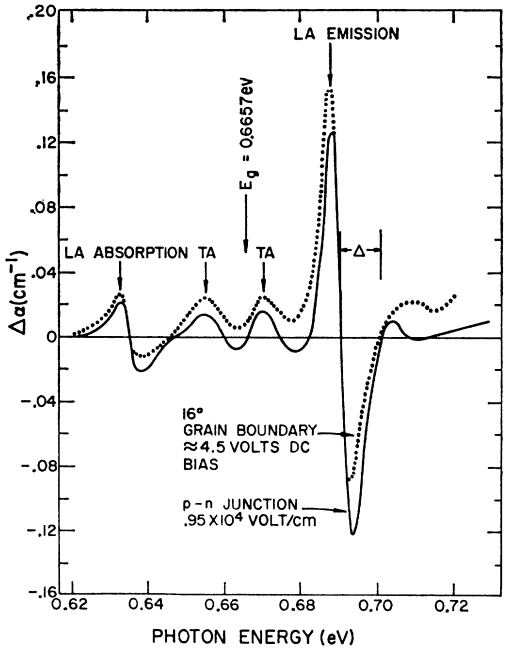

FIG. 7. Electrical-modulation results for 16° germanium bicrystal and germanium p-n junction showing similarity of indirect transition spectra obtained.

In the p-n junction measurements one finds

$$\Delta\propto(V+\Phi)^{\beta},$$

where β is roughly $\frac{1}{3}$, as shown in Fig. 8, and Φ is the diffusion potential. This implies

$$F\propto(V+\Phi)^{1/2},$$

as expected for a Schottky barrier junction. For the grain boundaries, one finds

$$\Delta\propto(V+\Phi)^{\beta},$$

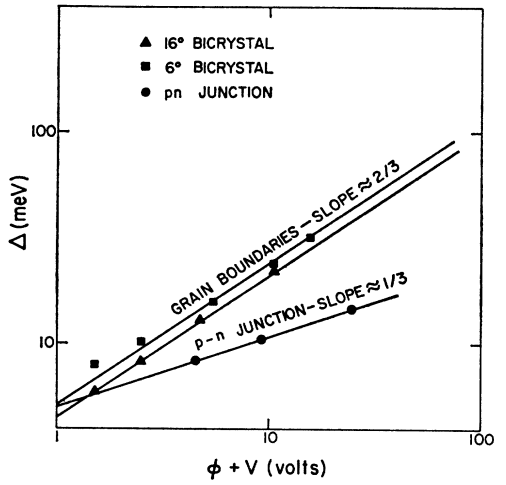

FIG. 8. Dependence of width of ≈0.69-eV oscillation on applied potential for grain boundaries and p-n junction.

where $\beta=\frac{2}{3}$, implying that the effective field in the grain-boundary space-charge layer goes as $\langle F\rangle \propto (V+\Phi)$. Since one of the p-n junctions is forward biased and one is reversed biased, the analysis will not be pursued further.

In all the electrical modulation measurements, there was no indication of any structure which could be assigned to the modulation of optical transitions involving the grain-boundary acceptor states.

IV. INTERPRETATION OF SPATIAL-MODULATION DATA

The above discussion shows that the bias-dependent component is due to electric-field-assisted absorption in the grain-boundary space-charge layer. In this section we discuss the origin of the bias-independent component which is the principal contributor to the absorption below 0.75 eV, as shown in Figs. 5 and 6. The good agreement between data from different samples and sample areas as mentioned in Sec. III indicates that the bias-independent component is a characteristic of the grain boundaries themselves. The most probable explanation for this component is states below the direct edge due to the lattice disorder. Other possibilities include absorption or scattering by impurities segregated at the boundaries, scattering by the grain layer, and effects of acceptor states. Each of these possibilities will be discussed.

The bias-independent absorption which we have assigned to boundary layer absorption varies over about 1.5 orders of magnitude in the range of our measurements ($\approx$0.55–$\approx$0.75 eV) in roughly exponential fashion. The exponential description appears to be a more accurate description as the tilt angle is increased. If we make the usual assumption that the energy dependence of the optical absorption is governed principally by the joint density of states, then these measurements imply that the grain-boundary layer joint density of states has, to a first approximation, an exponential dependence on photon energy $\hbar\omega$ below the bulk single-crystal direct edge at 0.80 eV. An exponential joint density of states follows from exponential band edges as indicated by the following simplified argument.

If the grain-boundary layer has conduction- and valence-band edges which have densities of states which are simple exponentials, then

$$\rho_C(E')=N_C\exp[-(E_C-E')/B_C],$$
$$\rho_V(E)=N_V\exp[-(E-E_V)/B_V],$$

where E_C and E_V are reference energies in the respective bands. For optical transitions, energy is conserved; therefore

$$E'=E+\hbar\omega.$$

The joint density of states is then given approximately by a convolution of the above densities which gives

$$\rho(\hbar\omega)\approx\exp(\hbar\omega/B_C)$$

under the assumptions that $B_C\approx B_V$ and the Fermi function can be taken as unity for $E\leq E_f$ and zero for $E>E_f$.

Such tails at band edges are sometimes attributed to compression (or dilation) regions connected with a disordered atomic arrangement. Dexter has discussed the absorption edge tails in insulating materials resulting from compression (or dilatation) zones around isolated edge dislocations.[29] Mott has recently presented a review which sums up current understanding of electronic behavior in disordered materials.[30] He points out that some of the states in the band tail may be localized and some nonlocalized with some critical energy E_L separating energy ranges in which states are localized from those which are not. Below E_L the density of states should fall off exponentially, whereas above E_L it should increase less rapidly. These propositions are generalizations from the results of several theoretical investigations of a preliminary nature.[30]

The similarity between the tail below the fundamental edge observed in our measurements and that predicted for disordered materials suggests that it would be fruitful to compare these results with those obtained on amorphous germanium. Clark[31] has measured optical absorption in thin amorphous germanium films of thickness up to 23 μ. Likewise Glass[32] has measured amorphous and polycrystalline films of about 5-μ thickness. Both find a simple exponential dependence of photon energy in the range 0.6–1.0 eV of the form

$$\alpha(\hbar\omega)=\text{const}\times\exp(\hbar\omega/B),$$

where measured values of B are 0.14 and 0.12, respectively. The measured values of α are uncertain by 10–15%.

These slopes compare with B values of 0.08 and 0.05 eV for fits of simple exponentials to the absorption data of the 16° and 20° tilt boundaries. In addition the magnitude of the absorption coefficient for amorphous germanium films is of order 5×10^2–5×10^3 cm^{-1} in the range 0.6–0.8 eV. These figures are in order-of-magnitude agreement with the values estimated for the grain-boundary layer absorption assuming a thickness of 100 Å or less.

Furthermore, the electrical properties of grain boundaries and amorphous germanium are somewhat similar. Both exhibit p-type conductivity with carrier concentrations of about 10^{17}–10^{18} carrier/cm^3.[7,33] However, the conductivity of amorphous germanium films is strongly temperature-dependent in contrast to the grain-boundary layer. This may indicate that in the former material

[29] R. M. Blakney and D. L. Dexter, in *Defects in Crystalline Solids* (The Physical Society, London, 1955), p. 108.
[30] N. F. Mott, Advan. Phys. **16**, 49 (1967).
[31] A. H. Clark, Phys. Rev. **154**, 750 (1967).
[32] A. M. Glass, Can. J. Phys. **43**, 1068 (1965).

$E_F > E_L$ while in the latter $E_F < E_L$. It should be noted at this point that not all investigators agree on the energy dependence of the optical absorption or on the conductivity properties for amorphous germanium. However, several recent studies show that the summary given above is basically correct, and that differences in optical properties may depend on preparation differences[34] and differences in conductivity may depend on variations of evaporation rate, aging, and annealing history.[35]

It is difficult to make definite statements from this comparison with amorphous germanium, a material which itself has not been well characterized either experimentally or theoretically. Nevertheless, we are impressed by the similarities between the grain-boundary-layer optical and electrical properties and those of the various amorphous films previously studied. The extent of this correspondence suggests that the "band structures" of these two materials are similar; namely, exponential densities of states into the energy gap away from the conduction- and valence-band edges as well as localized, intrinsic acceptor states close to (or within) the valence band which trap about 10^{18} cm^{-3} electrons in equilibrium at room temperature.

A. Scattering from the Boundary

The grain-boundary layer has a thickness of order 10^2 Å. The measured values of $\langle\langle\Delta\alpha\rangle\rangle\tau$ in the region where the bias-independent absorption predominates range from 10^{-4} to 10^{-3}. Hence $\langle\langle\Delta\alpha\rangle\rangle$ is of order 10^2–10^3 cm^{-1}. Furthermore, α for the single-crystal regions varies from 0 at 0.60 eV to 90 cm^{-1} at 0.75 eV while $\langle\langle\Delta\alpha\rangle\rangle$ ranges from about 10^2 cm^{-1} at 0.60 eV to about 10^3 cm^{-1} at 0.75 eV. Thus, we see that we can put

$$\alpha_{GB} \approx \langle\langle\Delta\alpha\rangle\rangle$$

and underestimate α_{GB} by less than 10%.

The attenuation coefficient for a substance is composed generally of two contributions: scattering out of the transmitted light beam and absorption

$$\alpha = \alpha_{scatt} + \alpha_{abs}.$$

We must first consider whether the measured grain boundary $\langle\langle\Delta\alpha\rangle\rangle\tau$ is a result of scattering by the grain-boundary layer. The wavelengths of light used here are of order 1 μ whereas the characteristic spacing d for any periodic variation of properties along the grain boundary (as in a dislocation array or fit-misfit model) is of order 100 Å. Thus, since $\lambda \gg d$, diffraction makes no contribution to α_{scatt} because the boundary layer probably has very uniform properties when averaged along the boundary for distances equal to λ.

The grain-boundary layer could be thought of as a narrow ($\approx$100 Å) film of index of refraction n' immersed in a medium (single-crystal region) of index n. The difference $n'-n$ might be as much as 5% of n. However, the fact that the wavelength is very much smaller than the thickness of the boundary layer, τ, will greatly diminish the effect of this difference. For the high angles of incidence on the grain boundary used in these studies, a fraction of the incident light could be reflected off the grain-boundary layer and in certain geometries out of the light beam collected by the detector. This possibility was explored experimentally by measuring spatial-modulation spectra with several beam-detector geometries, including geometries in which this "reflected" light would be collected by the detector. Variation of up to 10% in the magnitude of $\Delta I/I$ and slight changes in line shape were observed. Since $\Delta\alpha_{GB}$ represents orders-of-magnitude change, these results indicate that this contribution to α scattering is small.

In the preceding discussion, we have tried to demonstrate that scattering should be unimportant at the wavelengths of interest based primarily on the fact that $\lambda \gg \tau$, d. Lack of definite information about medium-angle grain-boundary structures makes it difficult to give quantitative proof of this contention; nevertheless, we feel that the foregoing qualitative considerations justify the neglect of α_{scatt}.

B. Possibility of Impurity Segregation

There is much experimental evidence that foreign atoms segregate at line defects. Cottrell[36] has shown that an impurity atom of radius different from that of the host material can relieve stresses in the vicinity of a dislocation. This interaction leads to a diffusion-limited migration of impurity atoms causing the formation of a "Cottrell atmosphere" of impurities in the region surrounding the dislocation.

However, Allen and Smith[37] have pointed out that in the case of a low-angle grain boundary ($<1°$) this interaction is less important. The cancellation effected by the overlap of the compressional and dilational regions around dislocations making up the low-angle grain-boundary array means that the range and strength of the interaction is much reduced. As pointed out earlier, the simple edge-dislocation array model probably does not apply for the medium-angle germanium grain boundaries examined in this study; nevertheless, the formation of impurity atmospheres is likewise attenuated because lattice disarray occurs only close to the grain-boundary plane.

The numerous experimental studies cited at the beginning of this article have repeatedly demonstrated

[33] R. Grigorovici, A. Devenji, and E. Teleman, in *Proceedings of the International Conference on Semiconductors, Paris, 1964* (Academic Press Inc., New York, 1964), p. 423.
[34] J. Wales, G. J. Lovitt, and R. A. Hill, Thin Solid Films **1**, 137 (1967).
[35] P. A. Walley and A. K. Jonscher, Thin Solid Films **1**, 367 (1968).
[36] A. H. Cottrell, *Dislocations and Plastic Flow in Crystals* (Oxford University Press, London, 1953).
[37] J. A. Allen and K. C. A. Smith, J. Electron **1**, 439 (1956).

that bicrystals doped with gallium, antimony, or copper in concentrations from 10^{14} to 10^{16} atoms/cm^3 show no dependence of grain-boundary electrical properties on impurity type or density. Moreover, there is no evidence of segregation of impurities in the vicinity of the grain-boundary layer. An experiment which bears particularly on this problem has been performed by Mueller.[13] By means of accurate capacitance measurements and analysis, he was able to measure the concentration of dopant, N_d, at the interfacial region between the grain-boundary layer and the grain-boundary space-charge layer for numerous bicrystals. The values of N_d measured in this way agreed within experimental accuracy with the values of N_d obtained from resistivity measurements on the single-crystal regions on either side of the boundary. The agreement between these values of N_d, one measured at $\lesssim$100 Å from the grain-boundary plane and one characteristic of regions far from the grain boundary, strongly supports the contention that no excess accumulation of electrically active impurities takes place in the vicinity of the grain boundary. On the basis of this evidence, we feel that the bias-independent optical absorption under discussion here cannot be ascribed to the effects of impurity segregation at the grain boundary.

C. Grain-Boundary Acceptor States

As pointed out earlier, the acceptor states have been shown to be intrinsic to the grain-boundary layer by a number of careful electrical measurements. If for the moment we consider crystalline germanium from the tight-binding approximation, each atom contributes four electrons to the bonding valence bands, of which there are four, all normally completely filled. If intrinsic acceptor states are to be formed (as at surfaces, grain boundaries, or in amorphous structures), then they must arise from electron levels or antibonding states "perturbed" out of the normally empty conduction bands.

Estimates from the electrical data give 10^{12}–10^{13} *filled* acceptor states per cm^2 of boundary area or approximately 10^{18}/cm^3 in the boundary layer. In terms of doping with a shallow impurity, this concentration corresponds to the heavily doped condition where an impurity band near the band edge can usually be observed optically. However, the temperature independence of the grain-boundary electrical properties strongly implies that these acceptor states lie below or within the tail on the valence band.

V. CONCLUSIONS

The technique herein called "spatial modulation" has been developed and applied to the study of optical absorption by medium-angle grain boundaries in n-type germanium bicrystals. The energy range covered was 0.55–0.80 eV. This method should be applicable to the study of optical absorption associated with any planar or inhomogeneous structure in a solid provided careful attention is paid to the effects of sample geometry and surface preparation.

The grain-boundary absorption has been shown to be composed of an electric-field-independent and an electric-field-dependent component. The field-independent component comes from absorption within the narrow grain-boundary layer (thickness less than 100 Å). Its characteristic "exponential" shape probably reflects the effects of lattice disorder in this region. Grain-boundary acceptor states may also contribute to the optical density of states but their effect should be relatively small. Since the problem of grain-boundary structure at medium angles remains undetermined, especially for covalent materials, no theoretical expression for the absorption coefficient can be derived for comparison with the data.

The field-dependent component is accounted for entirely by indirect and direct electric-field-assisted transitions in the grain-boundary space-charge layer (thickness of the order of microns). Electrical modulation of the grain-boundary absorption has yielded indirect and direct transition spectra nearly identical to those already observed in thick germanium p-n junctions.

In all these measurements the spectra obtained for the 6°31′ twist boundary was essentially indistinguishable from those obtained for tilt boundaries.